POLITECNICO
MILANO 1863

SCUOLA DI INGEGNERIA INDUSTRIALE
E DELL'INFORMAZIONE

Executive Summary of the Thesis

Risk Assessment of Uncontrolled Releases of Hydrogen and Methane Mixtures in Existing Methane Distribution Pipelines using CFD Simulations and Analytical Calculations

Laurea Magistrale in Chemical Engineering - Ingegneria Chimica

Author: Andrea Atzori

Advisor: Prof. Riccardo Mereu

Co-advisor: Marco Pontiggia

Academic year: 2022-2023

1. Introduction

In light of the escalating concerns associated with climate change, this study delves into the potential of hydrogen as a sustainable energy vector, placing a significant emphasis on the utilization of existing methane pipelines for hydrogen distribution. Acknowledging the inherent risks linked to potential uncontrolled releases from pipelines that transport a hydrogen and methane mixture, a dual strategy is introduced. This strategy encompasses the development of innovative analytical models alongside the application of computational fluid dynamics (CFD) simulations. The primary focus of these simulations is to examine the effects of physical obstructions on the expansion of the lower flammability limit cloud in mixed gas releases and to assess the characteristics of potential explosions. The derived data is aimed at enhancing safety measures, thereby contributing to more efficient and environmentally conscious strategies for energy transition.

The incorporation of hydrogen into the energy matrix might become very important for environmental sustainability, especially due to its capability of producing zero-emission energy across various sectors. A brand new approach towards decarbonization is proposed, involving the use of pre-existing methane pipelines for hydrogen distribution, which promises a cost-effective and smoother transition away from traditional fossil fuels.

However, the increased integration of methane pipelines comes with its risks [23][25][24][13][14]. Uncontrolled methane releases, which carry the potential for ignition and substantial harm, are further complicated by the presence of possible high-pressure jets, coming from potential ruptures, and physical obstructions that affect the dispersion of the gas cloud. Basic open-field modelling techniques are insufficient for capturing these complex dynamics, highlighting the need to consider real-world obstacles in these scenarios. To navigate these complexities, this research adopts a two-pronged approach: creating new analytical models and using advanced CFD simulations. These analytical models, formulated specifically for this study, provide an idealized representation of various release scenarios under different conditions. Conversely, the advanced CFD software enables precise sim-

ulation of the influence of realistic obstacles within potential release scenarios, including the structural complexities typical of distribution networks.
The primary objective of this research is to use aforementioned analytical models to theoretically describe the various release scenarios and then to employ CFD simulations to offer a realistic and analog perspective. By comparing these two approaches, the aim is to better understand the impact of obstructions on the expansion of the lower flammability limit cloud and the potential implications of these releases. The central aim is to exploit the power of CFD simulations to elucidate the impact of obstructions on the spread of the lower flammability limit cloud and to compare these insights with current analytical models. In doing so, the research seeks to clarify the possible implications of releases within these environments. The importance of CFD modelling takes center stage, providing critical data to develop safer, more efficient, and environmentally conscious energy transition strategies.

2. Background

2.1. Jets in Literature

The study of under-expanded jets has a rich history, and their structure is now well-understood due to extensive research [8]. This knowledge is crucial in practical engineering applications such as aircraft exhaust and industrial releases, including accidental leakage of pressurized fluids [19][20]. Recently, the focus in industrial safety has shifted towards the study of impinging jets. The presence of an obstacle is significant for risk evaluation, yet there is a lack of detailed studies on jet interaction with obstacles [27][12][3][10][1][7][26][5][16].

2.2. Free Jet

A free jet is unaffected by environmental interactions, meaning it doesn't interact with the ground, walls, or obstacles. The concentration profile within a jet, whether subsonic or supersonic [5][4], changes with axial and radial positions due to turbulence and entrainment effects. The decay of the mean mole fraction of the released substance can be expressed as follows:

$$\bar{\eta} = \frac{KD}{x+a}\sqrt{\left(\frac{\rho_{air}}{\rho_{gas}}\right)} \tag{1}$$

In this equation, D represents the orifice diameter, K is the decay constant, a is the displacement relative to the source, ρ_{air} and ρ_{gas} are the densities of air and gas, and x is the axial coordinate of the jet.

2.3. Jet in Presence of Obstacles

Studies on jets, including vertical, horizontal, and impinging near surfaces, show that when a gas discharge is directed towards large obstacles, an impinged jet is expected. This results in a sudden drop in gas velocity, reducing air entrainment and increasing damage distances [19].

2.4. Jet's Structure

An under-expanded supercritical jet occurs when the fluid pressure at the orifice is greater than twice the ambient pressure. The jet structure is influenced by compressible and viscous effects [29]. The Nearfield zone comprises the core and mixing layer regions. In the core, compressible effects dominate, followed by isoentropic expansion and re-compression through shock waves.

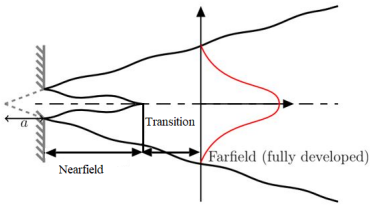

Figure 1: Jet Zones Subdivision.

The mixing layer features turbulence and large eddies, leading to a homogenization of the pressure field in the Transition zone. The Fairfield zone represents the fully expanded jet, where flow characteristics achieve similarity [29][16].

2.5. Models Classification

The behavior of a release in the atmosphere can be distinguished into three phases: Inertial, Buoyancy, and Dispersion. Initially, inertial forces dominate, then buoyancy forces take over, and finally, turbulent mixing in the atmosphere leads to an increase in jet dimensions. The mathematical models for jets can be classified

into Gaussian Models, Integral Models (Tube Flow), and CFD Models [11]. Gaussian Models are simple but limited [17], Integral Models offer more accuracy but have limitations in complex geometries, and CFD Models, though most accurate, demand substantial computational resources and expertise.

2.6. CFD Modelling for Safety Applications

CFD modelling has become more accessible for safety analysis and risk evaluation due to advancements in computing. Recent studies have focused on high-pressure methane jets, analyzing the effects of the ground on the Lower Flammable Limit zone and different models for the Equivalent Diameter. These studies highlight the growing importance and application of CFD in complex safety-related scenarios [19][6][15][2][21].

3. Materials and Methods

The approach to solving problems using Computational Fluid Dynamics (CFD) can be categorized into three main sections:

- Pre-processing.
- Solution.
- Post-processing.

The most commonly used CFD approach for industrial problems is the Reynolds-Averaged Navier-Stokes (RANS) method. RANS predicts the flow field behavior by averaging its point values over time. All simulations in this work are based on RANS simulations.

3.1. RANS Equations

Turbulent flow fields can theoretically be described by solving the full Navier-Stokes equations, starting with the continuity equation and coupling it with momentum, energy, and species equations, along with constitutive laws such as Fick's and the Equation Of State (EoS). Solving RANS equations requires a closure technique to compute these values.

Several turbulence models are available in ANSYS FLUENT®, including:

Standard k - ϵ: A two-equation model based on transport equations for the turbulence kinetic energy (k) and turbulent dissipation rate (ϵ).

Renormalization-group (RNG) k - ϵ: A model that addresses some issues of the standard k-ϵ model. It has a modified formulation for turbulent viscosity and a modified transport equation for the turbulent dissipation rate (ϵ).

Realizable k - ϵ: This model satisfies certain mathematical constraints on the Reynolds stresses, providing benefits in predicting the spreading rate of both planar and round jets.a

Standard k - ω: An empirical model based on transport equations for the turbulence kinetic energy (k) and the specific dissipation rate (ω), the ratio of ϵ to k.

k - ω Shear Stress Transition (SST): A hybrid model blending the Standard k - ϵ for high Reynolds number regions and Standard k -ω for low Reynolds number regions, suitable for a wide range of fluid flows.

3.2. Turbulence Model: k - ω SST

To address the closure problem in Reynolds Stress Tensor, the k - ω SST model was chosen among the various models [22].

3.3. Equivalent Diameter Approach

Several approaches exist to model the source of high-pressure under-expanded jets. The equivalent diameter approach used in this study is based on mass conservation, assuming no entrainment of ambient air, between the exit plane and a hypothetical point where the flow has the same pressure and temperature as the ambient fluid and is at sonic velocity.

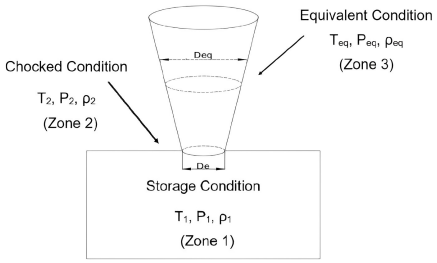

Figure 2: Equivalent Diameter Approach [4].

The assumption simplifies modelling by avoiding the initial zone of the supercritical jet where shock waves are present. Mass conservation between the original orifice and the pseudo-orifice allows for the following equations:

$$V_{eq} = \sqrt{\frac{\gamma R T_{eq}}{M_w}} \tag{2}$$

$$\rho_{eq} = \frac{P_{eq}}{RT_{eq}} \tag{3}$$

$$T_{tot} = T_{eq} + \frac{V_{eq}^2}{2 * C_p} \tag{4}$$

It is assumed that the equivalent temperature equals the ambient temperature, and the equivalent pressure equals the ambient pressure.

$$T_{eq} = T_{\infty} \tag{5}$$

$$P_{eq} = P_{\infty} \tag{6}$$

where,

- V_{eq} is the velocity at the Equivalent Diameter.
- γ is the heat capacity ratio.
- R is the universal gas constant.
- M_w is the molecular weight.
- ρ_{eq} is the density at the Eq. Diameter.
- T_{eq} is the temperature at the Eq. Diameter.
- P_{eq} is the pressure at the Eq. Diameter.
- C_p is the specific heat capacity at constant pressure.
- T_{tot} is the Stagnation temperature.

The Equivalent Diameter is calculated as

$$d_{ps} = d\sqrt{C_d \frac{V_2}{V_{eq}} \frac{\rho_2}{\rho_{eq}}} \tag{7}$$

where

- V_2 is the velocity in zone 2.
- C_d is the discharge coefficient.
- ρ_2 is the density in zone 2.
- d is the real diameter of the source.

3.4. ANSYS® Simulation Software

Computational Fluid Dynamics (CFD) is essential for simulating fluid interactions with complex surfaces and predicting fluid behavior in various scenarios. The ANSYS® 2022 software suite plays a crucial role in CFD simulations with its comprehensive tools:

- **ANSYS® Workbench** is the central interface, integrating various software tools for an efficient workflow. It facilitates project management, from geometry design to result visualization.
- **ANSYS® SpaceClaim** is a 3D modeling tool for designing complex geometries, offering flexibility and speed in the initial simulation stages.
- **ANSYS® Fluent Meshing** handles mesh creation for complex geometries, balancing computational efficiency and simulation accuracy.
- **ANSYS® Fluent** is a state-of-the-art solver for tackling complex CFD problems, leveraging parallel processing for speed and accuracy.
- **ANSYS® CFD-Post** is used for post-processing, analyzing and visualizing simulation results from Fluent.

3.5. Analytical Approach

3.5.1 The CSTR Model

A detailed analysis was conducted using a Microsoft Office Excel worksheet, drawing physical data from Phast™ software. Key parameters included the diameter of the rupture hole, input temperature and pressure, peak release pressure of the hydrogen and methane mixture, jet velocity, and upper and lower flammable limits (UFL and LFL).

The Continuous Stirred-Tank Reactor (CSTR) model was adapted for this study, focusing on the accumulation of the mixture over time. The balance equation in the CSTR model accounted for the concentration of hydrogen-methane mixtures within a control volume, considering inlet flowrates of ventilated air and the released mixture, and outlet flowrates of mixed flows.

Assumptions for the model included perfect mixing, a defined control volume, and constant fluid density. The data from Phast™ was used to calculate release flux and natural ventilation inlet flux, essential for determining the total inlet flux for the balance equation. Concentration profiles over time were generated to monitor the evolution of the mixture and define the flammability window for various compositions and scenarios.

3.6. The GAME Project

The GAME project enhances the Multi-Energy Method (MEM) for analyzing vapor cloud explosions, focusing on improving overpressure estimation. Its objective is to provide detailed guidance on selecting source strength, crucial for accurate blast parameter determinations, thus improving safety in operations prone to vapor cloud explosions.

The project utilizes advanced computational methodologies to assess energy release in var-

ious scenarios, a key factor in calculating the explosion radius. It also addresses complex scenarios such as non-central ignition locations and non-cylindrical obstacle configurations, offering practical solutions while noting some uncertainties.

Phast^{TM} software is used in the project for overpressure analysis, which is critical in predicting the extent of damage from explosions. The project examines various cases, including the failure of reinforced concrete at 300 mbar, steel structures at 170 mbar, and glass breakage at 20 mbar, to understand the interplay between overpressure, explosion radius, and resultant damage.

For open scenarios with low ignition energy, the project uses the following equation for explosion overpressure calculation:

$$P_0 = 0.84 * (VBR * L_p/D)^{2.75} * S_L^{2.7} * D^{0.7} \quad (8)$$

This equation incorporates the volume blockage ratio (VBR), flammable path length (L_p), diameter (D), and laminar burning velocity (S_L) of the mixture.

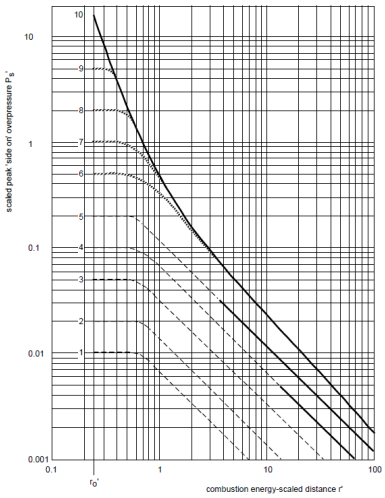

Figure 3: Blast chart MEM for overpressure.

Figure 3 showcases the MEM blast chart, used to determine peak blast overpressure based on combustion energy. It involves calculating the scaled distance (r') and deriving actual overpressure (P_s) from the scaled blast overpressure (P'_s) multiplied by ambient overpressure (p_0). The overpressure calculation, particularly for scaled distances smaller than a specific threshold, is vital for selecting the appropriate line on the blast chart [28].

4. Scenarios

4.1. Scenario 1

An accidental discharge from a subsurface conduit (with no surrounding walls), typically caused by external activities like excavation. This scenario is hypothesized as a ground-level discharge in a confined volume and is analyzed using analytical methods.

4.2. Scenario 2

An accidental rupture in a pressure reduction facility in an urban environment. The scenario evaluates the impact of the varying hydrogen concentrations in Natural Gas and Hydrogen (NGH2) blends on operational and safety parameters.

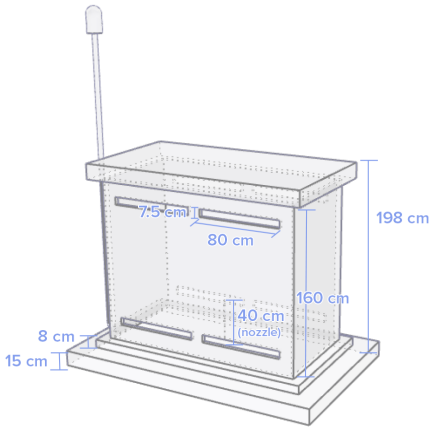

Figure 4: Detail of the GRFD cabin in Sc.2.

4.3. Scenario 3

An unexpected release in a REMI cabin, part of a gas distribution network. The study investigates the potential for explosive and flammable mixtures formation in this confined space, considering the impact of hydrogen concentrations.

4.4. Scenario 4

A rupture in an underground well of a reduction facility, naturally ventilated. The scenario assesses again the formation of hazardous mixtures with varied hydrogen levels in the NGH2 blend.

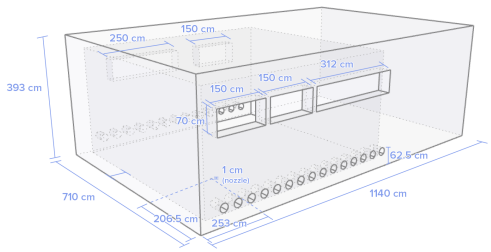

Figure 5: Perspective drawing of Scenario 3.

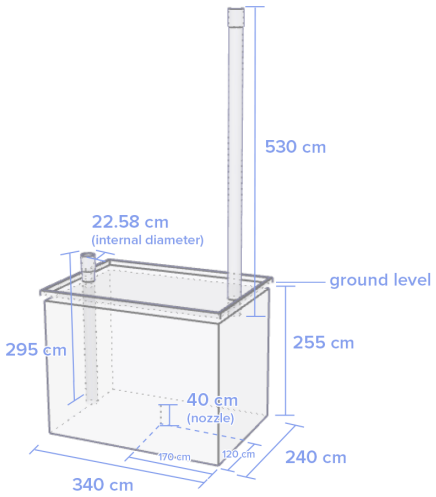

Figure 6: Perspective drawing of Scenario 4.

5. Data and parameters

	Sc.1	Sc.2	Sc.3	Sc.4
CV	7.5 m^3	3.84 m^3	313.108 m^3	20.808 m^3
HD	80 mm	8 mm	8 mm	8 mm
P	12 bar	5 bar	75 bar	50 bar
T	20°C	20°C	20°C	20°C
AF	0.011 m^3/s	0.053 m^3/s	0.785 m^3/s	0.011 m^3/s

Table 1: Defining Parameters of the Different Scenarios (CV = Control Volume, HD = Hole Diameter, P = Pressure, T = Temperature, AF = Air Flowrate).

Initial parameters for calculations, including NGH2 blends and peak flowrates are reported in this section. Weather conditions for gas dispersion are categorized as D5, indicating neutral atmospheric stability. The study considers a range of five hydrogen molar compositions in NGH2 blends, from 0% to 100%.

Molar H_2 %	Sc.1	Sc.2	Sc.3	Sc.4
0%	9.84	0.044	0.62	0.4
10%	9.39	0.042	0.58	0.38
20%	8.92	0.040	0.55	0.36
40%	7.91	0.036	0.47	0.32
100%	3.50	0.016	0.20	0.14

Table 2: Release peak flowrates in the different studied cases. The values are measured in [kg/s].

Moreover, Table 3 presents the Lower Flammability Limit (LFL) and Upper Flammability Limit (UFL) values for the blend composed of air, methane, and hydrogen, illustrating how these values vary according to variations in the hydrogen composition in terms of volumetric concentration. [18][9]

H_2 %	0%	20%	30%	40%	100%
LFL	0.04	0.04	0.04	0.04	0.04
UFL	0.17	0.18	0.20	0.24	0.75

Table 3: Flammability limits [vol/vol] for the different blends.

6. CSTR model approach

6.1. Flammability windows

Uses the Continuous Stirred-Tank Reactor (CSTR) model to calculate NGH2 mixture concentration profiles within specified flammability windows.

$$C_{mix}(t) = C_{mix}^{IN}\left(1 - e^{-\frac{Qt}{V}}\right) \tag{9}$$

$$C_{mix}^{\%}(t) = \frac{C_{mix}(t) - LFL}{UFL - LFL} \tag{10}$$

Concentration profiles over time are studied for each scenario within their flammability windows, taking into consideration residence time in the different control volumes.

Molar H_2 %	Sc. 1	Sc. 2	Sc. 3	Sc. 4
0%	0.07 s	9 s	50 s	43 s
10%	0.07 s	9 s	55 s	46 s
20%	0.08 s	10 s	61 s	50 s
40%	0.09 s	12 s	75 s	59 s
100%	0.25 s	48 s	429 s	157 s

Table 4: Variance of residence time (in seconds) within the flammability window in the different cases.

Considering the variability of residence time within the flammability window as shown in Table 4, it is observed that this variation does not significantly impact the conditional probability of explosion. The data suggests that the differences in residence time are not substantial enough to notably alter the explosion risk.

6.2. GAME Project Approach

The TNO Multi Energy model, integral to evaluating Vapor Cloud Explosions (VCEs), effectively links an explosion's peak overpressure with the energy in the gas or vapor cloud. This link is vital for understanding the dynamics and potential consequences of VCEs, aiding in developing better safety measures and infrastructural designs. A detailed graph analysis reveals a convergence of certain curves for combustion energy-scaled distance values greater than 1, indicating a uniform trend in explosion strength under specific conditions (Figure 7).

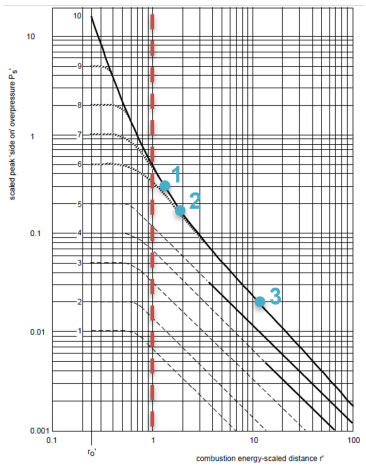

Figure 7

In analyzing hydrogen's influence, the study focuses on curve 10, known as the 'blast curve', which accurately represents high-strength explosions in confined spaces. This curve is particularly relevant for our scenarios. The study considers three critical limit values for overpressure: 300 mbar (leading to mortality and failure of reinforced concrete structures), 170 mbar (onset of mortality and failure of steel structures), and 20 mbar (reversible injuries and glass breakage). The variation in peak pressure, influenced by hydrogen concentration in the mixture, is captured in Equation 11:

$$P_{\%} = \frac{S_{L,mixture}^{2.7}}{S_{L,methane}^{2.7}} - 1 \tag{11}$$

This equation delineates the variations in peak pressure in relation to pure methane, due to the introduction of hydrogen into the mixture ($P_{\%}$), where S_L is laminar flame speed of the blend in cm/s [28]. Table 5 shows this variation, indicating that higher hydrogen concentrations lead to increased peak pressures, assuming consistent geometrical characteristics of the congested area.

Molar H_2 %	Mass H_2 %	S_L [cm/s]	P %
0%	0 %	37.2	0 %
10%	1.4 %	40.1	22 %
20%	3.0 %	43.9	56 %
40%	7.7 %	54.4	179 %
100%	100 %	285	24313 %

Table 5: Variations in peak pressure.

The study also involves calculating the Higher Heating Value (HHV) for different blend compositions, crucial for accurately determining the explosion radius. The HHV values (in $[MJ/kg]$ and $[MJ/m^3]$) for every studied blend composition have been calculated using the following formula, being X_{H2} the mass composition of hydrogen in the mixture and ρ_{mix} the density of the mixture in kg/m^3 for every studied case (Table 6).

$$HHV_{mix,mass} = X_{H2} * HHV_{H2} + (1 - X_{H2}) * HHV_{CH4} \tag{12}$$

$$HHV_{mix,vol} = HHV_{mix,mass} * \rho_{mix} \quad (13)$$

Molar H_2 %	Mass H_2 %	HHV_{mix} [MJ/kg]	ρ_{mix} [kg/m^3]	HHV_{mix} [MJ/m^3]
0%	0 %	55.5	0.66	37
10%	1.4 %	56.7	0.60	34
20%	3.0 %	58.1	0.54	32
40%	7.7 %	62.2	0.43	27
100%	100 %	141.8	0.08	12

Table 6: Higher Heating Values for different hydrogen blend compositions.

Furthermore, the explosion radius for different overpressure scenarios and hydrogen concentrations is calculated. As seen in Table 7, the radius of overpressure decreases with increasing hydrogen, suggesting that variations in hydrogen concentration do not significantly alter the explosion risk. This finding implies that existing safety procedures in natural gas facilities are adequate for managing risks associated with hydrogen blend variations.

	Molar H_2 %	Distance @300 mbar	Distance @170 mbar	Distance @20 mbar
Sc.2	0 %	15 m	21 m	129 m
	10 %	15 m	21 m	126 m
	20 %	14 m	20 m	123 m
	40 %	14 m	19 m	116 m
	100 %	10 m	15 m	89 m
Sc.3	0 %	65 m	92 m	561 m
	10 %	64 m	90 m	548 m
	20 %	62 m	87 m	534 m
	40 %	59 m	83 m	504 m
	100 %	45 m	63 m	384 m
Sc.4	0 %	26 m	37 m	227 m
	10 %	26 m	36 m	222 m
	20 %	25 m	35 m	216 m
	40 %	24 m	33 m	204 m
	100 %	18 m	25 m	155 m

Table 7: Explosion radius under different overpressure values for various scenarios.

Overall, the study reinforces the effectiveness of current safety strategies, even with an increased presence of hydrogen in gas mixtures.

6.3. Setting up ANSYS® Fluent

Various Equation of State (EoS) models are available in ANSYS® Fluent, such as Incompressible Ideal Gas Law, Ideal Gas Law for Compressible Flow, and others. The primary focus was on the Incompressible Ideal Gas Law model. For wind conditions, a uniform speed of 5 m/s was adopted. Specifically, in the third scenario, three different wind directions were examined (Figure 8). This addition gives a more realistic and complex aspect to the simulations, allowing for a deeper investigation of the case.

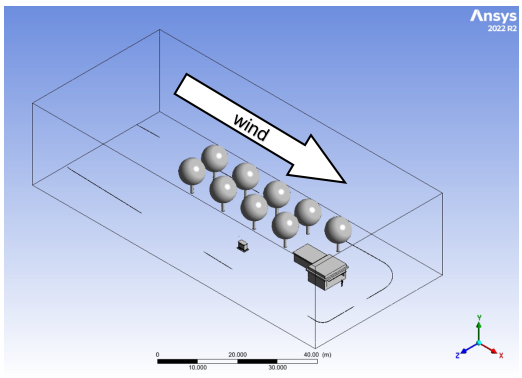

Figure 8: Wind direction in Scenario 2.

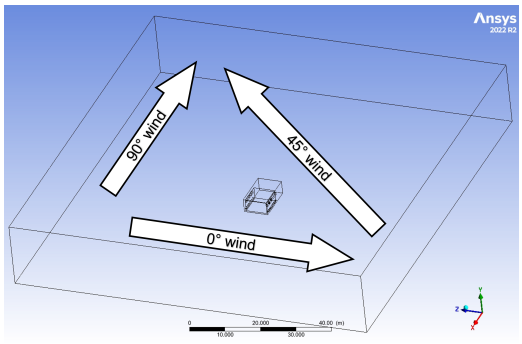

Figure 9: Wind directions in Scenario 3.

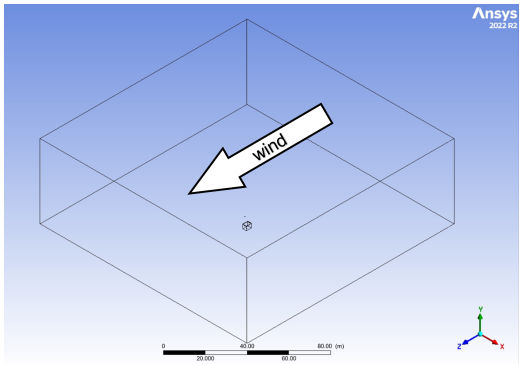

Figure 10: Wind direction in Scenario 4.

Regarding wall conditions, Fluent's standard parameters were used for most walls. However, for surfaces forming the enclosure, free-slip wall conditions were applied, simulating a more realistic scenario by considering the absence of friction or shear stress on these surfaces.
ANSYS® Fluent was configured for steady-state conditions using a pressure-based solver. Settings for the simulations are detailed in Table 8. Variations in settings include NGH2 mass flow rate and blend composition, based on the different scenarios.

Solution Method	**Scheme**
Pressure-velocity coupling	Coupled – pseudo transient
Spatial discretisation	**Scheme**
Gradient	Least square cell based
Pressure	Second order
Density	Second order upwind
Momentum	Second order upwind
Turbulent kinetic energy	Second order upwind
Energy	Second order upwind
Specific dissipation rate	Second order upwind
Other settings	
Gravity	-9.81 m/s^2 along y-direction
Iterations	Until convergence criteria is reached
Initialisation scheme	Hybrid

Table 8: ANSYS® Fluent settings.

This setup ensures a comprehensive and realistic simulation of fluid dynamics under various environmental conditions, enhancing the accuracy and applicability of the results.

6.4. Mesh

A concise and effective mesh was crucial for accurate CFD calculations. Using ANSYS® Fluent Meshing, a mesh suitable for the study was created. Key parameters included a progressive volumetric growth pattern (rate ≤ 1.2), starting from a millimetric cell size near the the release nozzle.
Surface Mesh settings involved a minimum size of 1 mm and a maximum size of approximately 3 m, with the growth rate consistently at 1.2. A boundary layer with standard parameters was added for a smooth mesh transition. For the Volume Mesh, tetrahedral cells were chosen due to the geometries' complexity, with a similar growth rate as the surface mesh, ensuring mesh accuracy and reliability.

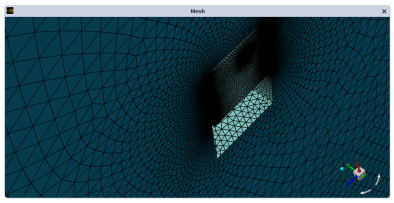

Figure 11: Detail of Scenario 3 mesh.

7. CFD simulations

To effectively analyze and contrast the results from Computational Fluid Dynamics (CFD) simulations with those obtained using Phast™, specific and significant indicators were selected. The focus was placed on measuring the downwind distance and the ground clearance of the plume of the NGH2 mixture cloud, at the Lower Flammability Limit (LFL) concentration.
These chosen parameters highlight how the CFD simulations, unlike the data taken from the Phast™ software, take into account the real-life constraints of the release scenarios. This includes realistic geometric configurations, the impact of turbulence in various situations, and the overall environmental context. Focusing on these aspects offers a deeper insight into the behavior of the NGH2 mixture cloud with different settings. Such an approach not only allows for a thorough comparison between CFD simulation data and existing data, but also enhances the accuracy and overall validity of the study.

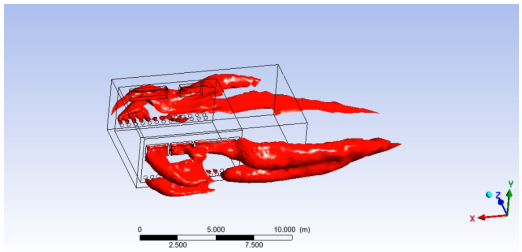

Figure 12: Scenario 3: LFL isosurface of pure hydrogen (90° wind).

The results obtained for different NGH2 blends are presented in Table 9. These results demonstrate notable differences compared to the data

obtained from Phast^{TM} simulations. To ensure an accurate comparison, specific assumptions were made based on the measurements taken. Crucially, the measurement of the plume's height from the ground provides a direct comparison point. The approach used to measure the downwind distance of the plume, however, varied depending on the specific geometry of each scenario. For Scenario 2, measurements were taken from the most distant point of the cabin openings. In Scenario 4, the measurement point was the downwind end of the highest ventilation opening. For Scenario 3, different approaches were used based on the wind direction. With wind directions of 0° and 45°, distances were measured perpendicularly from the downwind window. For a 90° wind direction, the methodology mirrored that of Scenario 2, measuring from the farthest endpoint relative to the wind direction.

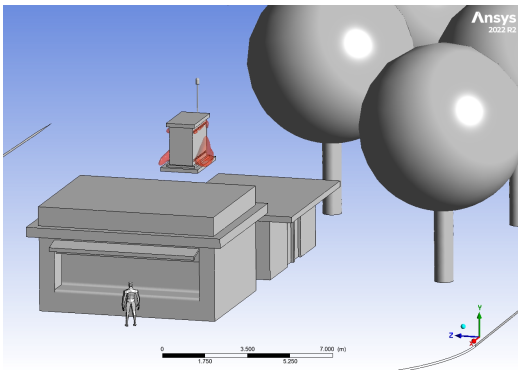

Figure 13: Scenario 2: LFL isosurface of pure methane.

The data shows how hydrogen, being lighter, produces a higher plume than methane. Interestingly, mixtures exhibit behaviors comparable to pure methane across scenarios. This consistency in the behavior of the flammability zone is crucial for the future of this application, signifying the potential for in-depth studies and affirming the analysis's success.
In summary, the disparity between the Phast^{TM} data (free jets) and Fluent CFD simulation results is largely due to the effect of containment on the NGH2 mixture, leading to pronounced turbulence and thorough mixing. Additionally, the interaction with wind, altered by the structure's aerodynamics, reduces the formation of flammable zones, a key factor for environmental preservation and risk assessment in future similar studies.

	H_2 %	DD [m]	GC [m]
Scenario 2	0%	0.49	1.90
	10%	0.45	2.00
	20%	0.43	1.89
	40%	0.41	2.06
	100%	1.67	2.36
Scenario 3 (0° wind)	0%	1.07	2.93
	10%	2.42	3.25
	20%	2.72	3.12
	40%	3.40	3.90
	100%	6.73	5.51
Scenario 3 (45° wind)	0%	3.64	3.32
	10%	2.97	3.01
	20%	2.65	3.54
	40%	2.59	3.43
	100%	6.44	3.71
Scenario 3 (90° wind)	0%	0.05	2.93
	10%	0.44	2.93
	20%	0.53	2.93
	40%	1.17	2.93
	100%	11.35	3.04
Scenario 4	0%	8.61	8.96
	10%	8.62	8.91
	20%	8.00	9.65
	40%	9.30	9.23
	100%	10.42	15.69

Table 9: Plume parameters calculated with ANSYS® Fluent (DD = Downwind Distance and GC = Ground Clearance).

8. Conclusions

- This thesis has conducted a thorough analysis of Vapor Cloud Explosions (VCEs), focusing on the behavior of different Natural Gas and Hydrogen (NGH2) blends. The study offers helpful insights for enhancing safety measures, response strategies, and infrastructural designs in the context of hydrogen combustion and VCEs.
- The research emphasizes the significance of understanding hydrogen combustion in VCEs. It has provided crucial data for safety measures and infrastructural design, particularly in calculating explosion radii for various NGH2 blends and scenarios, fa-

cilitating comparisons and deeper understanding of their implications.

- According to CEI EN 60079-10-1, gas mixtures with 30% or more hydrogen by volume should be considered as Group IIC or IIB+H2. This research confirms that existing procedures and personal protective equipment (PPE) for natural gas (NG) facilities are sufficient for such mixtures. Additionally, current detectors, unless specified otherwise, may require threshold adjustments for lower NG quantities due to their non-ignition risk for the flammable mixture.
- The study has contributed significantly to understanding the behavior of different fluid mixtures. It reveals that hydrogen and methane exhibit similar behaviors in certain contexts, laying a foundation for future research in this area.
- The research has provided a nuanced understanding of flammability zones, with significant implications for safety measures, risk assessments, and future scenario design. The minimal variation in these zones across different scenarios validates the reliability of the CFD simulations and their broader applicability.
- The successful outcomes of this study demonstrate the efficacy of Computational Fluid Dynamics (CFD) as a tool for analyzing complex fluid dynamics, highlighting its capability to produce reliable, reproducible, and insightful data.
- The findings highlight hydrogen's potential as a sustainable energy vector. The simulations provide insights into hydrogen's behavior under various conditions, crucial for its safe and efficient use. These might have significant implications for environmental sustainability and energy security, contributing in our ability to address environmental challenges.

References

[1] Benjamin Angers, Ahmed Hourri, Pierre Bénard, and Andrei V Tchouvelev. Numerical investigation of a vertical surface on the flammable extent of hydrogen and methane vertical jets. 2011.

[2] Pierre Bénard, Ahmed Hourri, Benjamin Angers, and Andrei Tchouvelev. Adjacent surface effect on the flammable cloud of hydrogen and methane jets: Numerical investigation and engineering correlations. *International Journal of Hydrogen Energy*, 41(41):18654–18662, 2016.

[3] Pierre Bénard, Ahmed Hourri, Benjamin Angers, Andrei V Tchouvelev, and VM Agranat. Effects of surface on the flammable extent of hydrogen jets. 2009.

[4] AD Birch, DR Brown, MG Dodson, and F Swaffield. The structure and concentration decay of high pressure jets of natural gas. *Combustion Science and technology*, 36(5-6):249–261, 1984.

[5] Ching Jen Chen and Wolfgang Rodi. Vertical turbulent buoyant jets: a review of experimental data. *NASA Sti/Recon Technical Report A*, 80:23073, 1980.

[6] Marco Derudi, Daniele Bovolenta, Valentina Busini, and Renato Rota. Heavy gas dispersion in presence of large obstacles: selection of modeling tools. *Industrial & Engineering Chemistry Research*, 53(22):9303–9310, 2014.

[7] Marie-Laure Ducasse, Julien Dubois, Muriel Amielh, and Fabien Anselmet. Experimental investigation of a turbulent variable density jet impinging on a sphere. In *Proceedings of the 15th international symposium on applications of laser techniques to fluid mechanics, Lisbon*, 2010.

[8] Erwin Franquet, Vincent Perrier, Stéphane Gibout, and Pascal Bruel. Free underexpanded jets in a quiescent medium: A review. *Progress in Aerospace Sciences*, 77:25–53, 2015.

[9] Eichert H. Gefaehrdungspotential bei einem verstaerkten Wasserstoffeinsatz. Deutsche Forschungsanstalt fuer Luft- und Raumfahrt (DLR), Stuttgart, Germany, 1992.

[10] Jonathan E Hall, Philip Hooker, L O'Sullivan, Benjamin Angers, Ahmed

Hourri, and P Bernard. Flammability profiles associated with high-pressure hydrogen jets released in close proximity to surfaces. *international journal of hydrogen energy*, 42(11):7413–7421, 2017.

[11] Nicholas S Holmes and Lidia Morawska. A review of dispersion modelling and its application to the dispersion of particles: an overview of different dispersion models available. *Atmospheric environment*, 40(30):5902–5928, 2006.

[12] A Hourri, B Angers, P Bénard, A Tchouvelev, and V Agranat. Numerical investigation of the flammable extent of semi-confined hydrogen and methane jets. *international journal of hydrogen energy*, 36(3):2567–2572, 2011.

[13] Hyung-Seok Kang, Sang-Min Kim, and Jongtae Kim. Safety issues of a hydrogen refueling station and a prediction for an overpressure reduction by a barrier using openfoam software for an sri explosion test in an open space. *Energies*, 15(20), 2022.

[14] SI Kim and Y Kim. Review: Hydrogen tank explosion in gangneung, south korea. In *Cent. Hydrog. Saf. Conf*, 2019.

[15] Jonathan G Koomey, Stephen Berard, Marla Sanchez, and Henry Wong. Web extra appendix: implications of historical trends in the electrical efficiency of computing. *IEEE Annals of the History of Computing*, 33(3):S1–S30, 2011.

[16] ANDREA MARTANI. Vertical cylindrical tank influence on high-pressure jets: a computational fluid dynamic study. 2019.

[17] Alberto Mazzoldi, Tim Hill, and Jeremy J Colls. Cfd and gaussian atmospheric dispersion models: A comparison for leak from carbon dioxide transportation and storage facilities. *Atmospheric environment*, 42(34):8046–8054, 2008.

[18] Zabetakis M.G. *Safety with cryogenic fluids*. Plenum Press, New York, 1967.

[19] M Pontiggia, Valentina Busini, M Ronzoni, G Uguccioni, Renato Rota, et al. Effect of large obstacles on high momentum jets dispersion. *Chemical Engineering Transactions*, pages 523–528, 2014.

[20] P.Salcher and J.Whitehead. Uber den aus uss stark verdichteter luft. sitzungsber,. *Akademie d. Wissenschaften Wien*, 1889.

[21] Luca Ragozzino. Methane high pressure jets ground interaction cfd analysis for safety purpose applications. 2017.

[22] PJ Richards and RP Hoxey. Appropriate boundary conditions for computational wind engineering models using the k-ϵ turbulence model. *Journal of wind engineering and industrial aerodynamics*, 46:145–153, 1993.

[23] Fotis Rigas and P Amyotte. Myths and facts about hydrogen hazards. In *13th International Symposium on Loss Prevention and Safety Promotion in the Process Industries, Florence, Italy (May 12-15, 2013)*, 2013.

[24] Fotis Rigas and Paul Amyotte. *Hydrogen safety*. CRC Press, 2012.

[25] Fotis Rigas and Spyros Sklavounos. Hydrogen safety. In *Hydrogen Fuel*, pages 547–580. CRC Press, 2008.

[26] RW Schefer, WG Houf, TC Williams, B Bourne, and J Colton. Characterization of high-pressure, underexpanded hydrogen-jet flames. *International journal of hydrogen energy*, 32(12):2081–2093, 2007.

[27] Christina F Sposato, WJ Rogers, and MS Mannan. Effects of obstacle geometry on jet mixing for releases of silane. In *Mary K O'Connor Process Safety Symposium. Proceedings 2000*. Mary Kay O'Connor Process Safety Center, 2000.

[28] WPM Werex, AC Van den Berg, and D van Leeuven. Application of correlations to quantify the source strength of vapour cloud explosions in realistic situations, final report for the project:'games'. *TNO report PML*, page C53, 1998.

[29] AJ Yule. Large-scale structure in the mixing layer of a round jet. *Journal of Fluid Mechanics*, 89(3):413–432, 1978.